

Non-Hermitian Hartman effect

Stefano Longhi^{1,*}

The Hartman effect refers to the rather paradoxical result that the time spent by a quantum mechanical particle or a photon to tunnel through an opaque potential barrier becomes independent of barrier width for long barriers. Such an effect, which has been observed in different physical settings, raised a lively debate and some controversies, owing to the correct definition and interpretation of tunneling times and the apparent superluminal transmission. A rather open question is whether (and under which conditions) the Hartman effect persists for inelastic scattering, i.e. when the potential becomes non-Hermitian and the scattering matrix is not unitary. Here we consider tunneling through a heterojunction barrier in the tight-binding picture, where the barrier consists of a generally non-Hermitian finite-sized lattice attached to two semi-infinite nearest-neighbor Hermitian lattice leads. We derive a simple and general condition for the persistence of the Hartman effect in non-Hermitian barriers, showing that it can be found rather generally when non-Hermiticity arises from non-reciprocal couplings, i.e. when the barrier displays the non-Hermitian skin effect, without any special symmetry in the system.

1 Introduction

Tunneling is one among the most peculiar and popular phenomena predicted by quantum mechanics [1]. The question of how much time a quantum particle takes to tunnel through a classically forbidden potential barrier is a rather old and somehow controversial topic in quantum physics [2–18], owing to the difficulty to find a unique and convincing definition of the tunneling time [17, 19–21] and the apparent superluminal transmission that is found in some cases [9, 13, 14, 16, 17]. The Hartman effect [3], i.e. the independence of the time delay for a quantum particle to tunnel across an opaque potential barrier, is perhaps one of the most intractable mysteries of tunneling that struggled physicists for more than

four decades [7, 9, 10, 14, 17, 22]. Measurements of tunneling times, including the demonstration of the Hartman effect and superluminal group delay times, have been reported in several experiments for electrons, photons and ultracold atoms [23–36]. The relevance of tunneling times has been discussed in several areas of physics, including electron tunneling ionization in atoms [19, 31–34], photon tunneling in microwave and optical barriers [23–30], tunneling of ultracold atoms [35–37] and electron tunneling in quantum superlattices and graphene [38–42]. It is now well understood that the group delay time can result in apparent superluminal propagation or even negative group velocities, without violating causality and relativity [13, 17, 35, 43]. For recent works discussing the various controversies and interpretations of the Hartman effect see, for example, the review article [15] and the more recent works [17, 22, 35, 43]. Most of previous results on the Hartman effect, with the exception of few works [44–50], concern with non-dissipative (Hermitian) systems, where the dynamics conserves the norm of the wave function and the scattering matrix is unitary. However, in dissipative (open) quantum systems as well as in a variety of classical platforms such as photonic systems, mechanical metamaterials and topoelectrical systems, scattering phenomena are described by effective non-Hermitian (NH) Hamiltonians, displaying non-unitary dynamics and possible singularities in the spectrum (see e.g. [51–56] and references therein). One class of such systems are those described by non-Hermitian Hamiltonians with parity-time (PT) symmetry, which were originally introduced in an attempt to generalize the theory of quantum mechanics beyond the usual Hermiticity paradigm [57, 58]. PT symmetry has become recently very popular and found several applications in photonics [52–55]. In PT systems, non-Hermiticity basically arises from a complex potential with balanced dissipative (lossy) and amplifying (gain) regions. More recently, a great interest has been devoted

* Corresponding author E-mail: stefano.longhi@polimi.it

¹ Dipartimento di Fisica, Politecnico di Milano, Piazza L. da Vinci 32, I-20133 Milano, Italy and IFISC (UIB-CSIC), Instituto de Fisica Interdisciplinar y Sistemas Complejos, E-07122 Palma de Mallorca, Spain

toward a different type of non-Hermitian systems displaying the so-called non-Hermitian skin effect [59–83], i.e. a strong sensitivity of the energy spectrum on the boundary conditions and the condensation of a macroscopic number of bulk states at the lattice edges under open boundary conditions [59–67]. Such non-Hermitian systems exhibit a rich and nontrivial band topology [60, 68, 71, 73, 80], which emerges rather generally from non-reciprocal hopping amplitudes induced by synthetic imaginary gauge fields [59, 84–89], rather than from complex on-site potentials. Lattices with effective non-reciprocal hopping amplitudes have been demonstrated in different physical systems, such as in photonic systems [76, 81, 82], topoelectrical circuits [78], mechanical systems [77] and ultracold atoms [83]. In particular, the use of synthetic lattices in frequency domain [81] can realize rather arbitrary single-band NH Hamiltonians with tailored non-reciprocal hopping displaying arbitrary topological winding numbers.

The impact of inelastic scattering on the tunneling times and Hartman effect has been investigated in few models [44, 45, 47–50], where non-Hermiticity was introduced via a complex potential term in the Hamiltonian. A general result is that, for a sufficiently strong absorption, the Hartman effect is washed out and the tunneling time turns out to depend on barrier width [44, 45, 47]; such a result is in agreement with some early observations on photon tunneling in microwave experiments [45]. On the other hand, the Hartman effect persists in PT symmetric complex potential barriers [49, 50], with alternating layers of absorption and gain, suggesting that PT symmetry can play a main role in preserving the Hartman effect under non-Hermitian scattering processes [50]. However, it is a fully open question whether PT symmetry is a necessary requirement for the observation of the Hartman effect in non-Hermitian scattering processes, and whether the Hartman effect can be observed under different types of non-Hermiticity, involving imaginary gauge fields [84–89], so beyond the PT symmetry paradigm.

In this work we address such main questions considering the problem of tunneling time for scattering in tight-binding lattices [90–96] where the barrier consists of a generally non-Hermitian finite-sized superlattice attached to two semi-infinite nearest-neighbor Hermitian lattice leads [92, 93, 96]. The main result is that under rather general conditions the Hartman effect persists in non-Hermitian models, also when the non-Hermitian barrier does not possess PT symmetry and there is the NH skin effect. The results are illustrated by considering tunneling across NH barriers described by the generalized Hatano-Nelson model and by a NH extension of the Rice-Mele model.

2 Transmission throughout a tight-binding non-Hermitian barrier: model and scattering analysis

We consider wave transmission through a non-Hermitian barrier on a one-dimensional (1D) tight-binding lattice, as schematically shown in Fig.1(a). Basically, we consider a tight-binding heterojunction where two semi-infinite tight-binding Hermitian chains (leads) with nearest neighbor hopping amplitude κ , providing the two scattering channels, are connected to the edge sites of a non-Hermitian barrier, which is described by a tight-binding superlattice containing N unit cells and M sites in each unit cell [Fig.1(a)]. Non-Hermiticity can be introduced by either (or both) complex on-site potentials V_1, V_2, \dots, V_M in the sites A_1, A_2, \dots, A_M of each cell or by non-reciprocal (asymmetric) hopping amplitudes. In the latter case the superlattice displays rather generally the NH skin effect [63], although it can be found in some models with reciprocal hopping as well [54].

To study the scattering properties of the non-Hermitian barrier, let us consider a Bloch wave $\sim \exp(-iqn)$ with wave number q and energy $E_0 = 2\kappa \cos q$, with a positive group velocity $v_g = -(dE/dq) = 2\kappa \sin q$ (i.e. $0 < q < \pi$), incident onto the barrier from the left side. Let us indicate by $H(\beta)$ the $(M \times M)$ matrix Hamiltonian in Bloch space of the superlattice in the barrier, with $\beta = \exp(ik)$. Clearly, in a lattice with short-range hopping the elements of the matrix Hamiltonian $H(\beta)$ are Laurent polynomials in β . The Bloch bands of the superlattice under periodic boundary conditions, $E_\alpha(k)$ ($\alpha = 1, 2, \dots, M$), are the M eigenvalues of the matrix Hamiltonian H with k real. Note that such energies are complex and, in the presence of the NH skin effect, they describe rather generally a set of closed loops $\mathcal{C}_1, \mathcal{C}_2, \dots, \mathcal{C}_M$ in complex energy plane [Fig.1(b)]. In analogy with the Hermitian case, we say that the barrier is opaque to an incident wave of energy E_0 whenever E_0 does not belong to none of the loops $\mathcal{C}_1, \mathcal{C}_2, \dots, \mathcal{C}_M$. In this case, the wave function in the barrier region is described by a suitable superposition of evanescent waves, i.e. with complex Bloch wave numbers. However, it should be mentioned that, unlike in Hermitian barriers, owing to the NH skin effect the evanescent nature of the waves in the barrier does not necessarily imply that such waves are not propagative.

To study wave scattering across the barrier, let us consider the determinant

$$\Delta(\beta, E_0) = \det(E_0 - H(\beta)) \quad (1)$$

which is a function of both β and energy E_0 of the incoming wave. As a function of β , $\Delta(\beta, E_0)$ is a Laurent

polynomial of the form

$$\Delta(\beta, E_0) = \sum_{l=-s}^r R_l(E_0) \beta^l \quad (2)$$

with some energy-dependent coefficients $R_l(E_0)$, where $s, r \geq 1$ are the largest orders of left (s) and right (r) hopping on the superlattice, respectively. The determinantal equation $\Delta(\beta, E_0) = 0$ thus yields a set of $(s+r)$ roots $\beta_1, \beta_2, \dots, \beta_{r+s}$, which for an opaque barrier are in modulus different than one. Therefore, in the barrier region the wave function is described by a superposition of evanescent waves which are either growing ($|\beta| > 1$) or decaying ($|\beta| < 1$) as the cell number n increases. We order the roots such that

$$|\beta_1| \leq |\beta_2| \leq \dots \leq |\beta_{s+r}| \quad (3)$$

and indicate by $U^{(1)}, U^{(2)}, \dots, U^{(s+r)}$ the associated eigenvectors of H , i.e. $H(\beta_l)U^{(l)} = E_0 U^{(l)}$. For a barrier of width N larger than $(r+s)$, the scattering solution ψ_n to the time-independent Schrödinger equation corresponding to the incoming wave of energy E_0 from the left side of the barrier can be written in the form

$$\psi_n = \begin{cases} \exp(-iqn) + \mathcal{R}(q) \exp(iqn) & n \leq 0 \\ \sum_{l=1}^{s+r} G_l U^{(l)} \beta_l^n & 1 \leq n \leq N \\ \mathcal{T}(q) \exp[-iq(n-N-1)] & n \geq N+1 \end{cases} \quad (4)$$

where $\mathcal{R}(q), \mathcal{T}(q)$ are the spectral reflection and transmission coefficients (for left incidence side) and G_l the amplitudes of evanescent waves in the barrier region. Note that ψ_n is a scalar for $n < 1$ and $n > N$, while it is a vector of size M in the barrier superlattice, containing the wave amplitudes in each site A_1, A_2, \dots, A_M of the n -th cell ($n = 1, 2, \dots, N$) of the barrier superlattice. The values of the $(s+r+2)$ variables $\mathcal{R}(q), \mathcal{T}(q), G_1, G_2, \dots, G_{r+s}$ are obtained by imposing the matching conditions at the two junctions. These include the two matching equations at sites $n = 0$ and $n = N+1$, in the leads, given by

$$E_0(1 + \mathcal{R}) = \kappa [\exp(iq) + \mathcal{R} \exp(-iq)] + \kappa \sum_{l=1}^{r+s} G_l U_1^{(l)} \beta_l \quad (5)$$

$$E_0 \mathcal{T} = \kappa \mathcal{T} \exp(-iq) + \kappa \sum_{l=1}^{r+s} G_l U_M^{(l)} \beta_l^N, \quad (6)$$

and other $(r+s)$ equations for the first s sites in the superlattice at the left edge, and the last r sites in the superlattice at the right edge. Such equations are linear in the amplitudes G_l with coefficients that contain the powers $\beta_l, \beta_l^2, \dots, \beta_l^{r+s}$ and $\beta_l^{N-s-r+1}, \beta_l^{N-s-r+2}, \dots, \beta_l^N$. The explicit form of such equations is given in the Appendix A for the special case of $M = 1$, while an illustrative example for $M = 2$ is given in Sec.4.2. The resulting system is a set

of $(s+r+2)$ linear and inhomogenous equations in the $(s+r+2)$ unknown variables $\mathcal{R}(q), \mathcal{T}(q), G_1, G_2, \dots, G_{r+s}$, which can be solved to determine the spectral transmission amplitude $\mathcal{T}(q)$.

3 Tunneling phase time and the non-Hermitian Hartman effect

The Hartman effect refers to the independence of the tunneling phase time (also referred to as the group delay time or Wigner time) on the barrier width for long opaque potential barriers [3, 9, 16, 17]. Here we do not enter into the rather longstanding and controversial question whether the phase time does provide an accurate estimate of the traversal time (see e.g. [16, 17] and reference therein), however we mention that such an independency of barrier width can be found for other types of mean tunnelling times [16] and that, according to Ref. [17], the group delay has a clear physical significance despite its interpretation as a traversal time cannot be justified. When dealing with wave tunneling in a non-Hermitian barrier, the phase time keeps its clear physical meaning as the delay time of the peak of a spatially-broad wave packet to escape from the barrier. This time can be readily measured in a tunneling experiment based, for example, on light propagation across NH photonic barriers [28, 29]. Other tunnelling times, such as the dwell time, could not be readily extended to non-Hermitian barrier tunneling or could not be defined uniquely. For example, in [46] it was shown that different dwell times can be introduced in non-Hermitian tunneling, and that one of them can become a complex number, with a nontrivial physical meaning.

In this section we aim at calculating the tunneling phase time in the scattering process of Fig.1(a), i.e. across a NH potential barrier in the tight-binding picture. Let us consider a spatially-broad wave packet incident onto the NH barrier from the left side with a spectral amplitude $F(\delta)$ very narrow at around the mean Bloch wave number $\delta = q$. For $n \leq 0$ the wave function can be written as the sum of the incident $\psi_n^{(inc)}(t)$ and reflected $\psi_n^{(ref)}(t)$ wave packets i.e. $\psi_n(t) = \psi_n^{(inc)}(t) + \psi_n^{(ref)}(t)$ with

$$\psi_n^{(inc)}(t) = \int d\delta F(\delta) \exp[-i\delta n - iE(\delta)t] \quad (7)$$

$$\psi_n^{(ref)}(t) = \int d\delta \mathcal{R}(\delta) F(\delta) \exp[i\delta n - iE(\delta)t] \quad (8)$$

while for $n > N$ the transmitted wave packet, on the right hand side of the barrier, reads

$$\psi_n^{(trans)}(t) = \int d\delta F(\delta) \mathcal{T}(\delta) \exp[-i\delta(n-N-1) - iE(\delta)t].$$

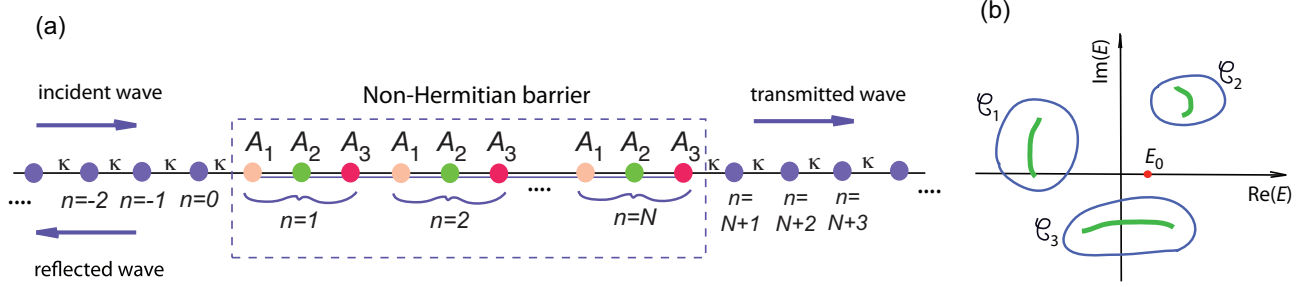


Figure 1 (a) Schematic of wave scattering across a non-Hermitian barrier in a tight-binding heterojunction. The barrier consists of a chain of N unit cells of a non-Hermitian superlattice, with M sites A_1, A_2, \dots, A_M in each supercell ($M = 3$ in the figure). The barrier is attached to two semi-infinite Hermitian tight-binding chains with nearest-neighbor hopping amplitude κ (leads). The index n denotes the number of the cell in the chain. (b) Energy spectrum of the superlattice under periodic boundary condition (solid curves). In the presence of non reciprocal hopping, the energy spectrum consists of a set of M closed loops $\mathcal{C}_1, \mathcal{C}_2, \dots, \mathcal{C}_M$ in complex energy plane ($M = 3$ in the figure) and the system displays the NH skin effect. The superlattice barrier is opaque for the incoming wave of energy $E_0 = 2\kappa \cos q$ on the real energy axis whenever E_0 does not belong to none of the closed loops. The bold open arcs internal to the closed loops correspond to the energy spectrum of the NH superlattice under OBC. The condition $|\beta_s| < |\beta_{s+1}|$ for the observation of the Hartman effect physically implies that the energy E_0 of the incoming wave should not belong to the OBC energy spectrum.

$$(9) \quad \text{where } \tilde{\varphi}(q) \text{ and } \varphi_{\beta_s}(q) \text{ are the phases of } \tilde{\mathcal{F}}(q) \text{ and } \beta_s(q), \text{ respectively.}$$

After letting $\mathcal{F}(q) = |\mathcal{F}(q)| \exp[i\varphi_t(q)]$, using the method of stationary phase [9, 16, 17] one can calculate the phase (group delay) time, from $n = 0$ to $n = N + 1$, which reads

$$\tau = \frac{(d\varphi_t/dq)}{(dE/dq)} = -\frac{(d\varphi_t/dq)}{2\kappa \sin q}. \quad (10)$$

Therefore, the tunneling phase time τ is basically established by the derivative of the phase of the spectral transmission amplitude. To establish whether the phase time becomes independent of N (the barrier width) in the large N limit, we use a main result, proved in Appendix B, for which in the large N limit the form of the spectral transmission coefficient $\mathcal{F}(q)$ reads

$$\mathcal{F}(q) = \tilde{\mathcal{F}}(q) \beta_s^N \quad (11)$$

where $\tilde{\mathcal{F}}(q)$ is independent of N . The above result holds provided that the inequality $|\beta_s| < |\beta_{s+1}|$ strictly holds, where $\beta_1, \beta_2, \dots, \beta_{r+s}$ are the $(s+r)$ roots of the determinantal equation $\Delta(\beta, E_0) = 0$ ordered according to Eq.(3). Interestingly, the condition $|\beta_s| < |\beta_{s+1}|$ for the validity of Eq.(11) implies that the energy E_0 of the incoming wave does not belong to the energy spectrum of the NH superlattice under open boundary conditions (OBC) (see [69, 73, 75, 97] and Appendix A).

From Eqs.(10) and (11) it readily follows that the phase time reads

$$\tau = -\frac{(d\tilde{\varphi}/dq)}{2\kappa \sin q} - N \frac{(d\varphi_{\beta_s}/dq)}{2\kappa \sin q} \quad (12)$$

where $\tilde{\varphi}(q)$ and $\varphi_{\beta_s}(q)$ are the phases of $\tilde{\mathcal{F}}(q)$ and $\beta_s(q)$, respectively. Therefore, we conclude that the necessary and sufficient condition for the Hartman effect to occur in the tunneling across the NH barrier is that the phase of the root β_s does not depend on q in the neighbor of the carrier Bloch wave number q of the incoming wave packet, i.e. that the stationarity condition $(d\varphi_{\beta_s}/dq) = 0$ is satisfied. This occurs, for instance, whenever $\beta_s(q)$ is a real number, and this condition can occur under rather broad selection of parameters, even without any symmetry in the system. For example, let us consider the case $M = 1$, so that $H(\beta)$ is a scalar and given by the Laurent polynomial

$$H(\beta) = \frac{t_{-s}}{\beta^s} + \frac{t_{-s+1}}{\beta^{s-1}} + \dots + t_0 + t_1 \beta + \dots + t_r \beta^r \quad (13)$$

where $t_{\mp l}$ are the left or right hopping amplitudes among sites distant $|l|$ in the lattice and $s, r \geq 1$ are the largest orders of left or right hopping. Such a single-band NH Hamiltonian could be implemented, for example, in photonics using a synthetic lattice in the frequency domain, where a ring resonator undergoes simultaneous phase and amplitude modulations that control the left and right hopping amplitudes in the lattice [81]. The system displays the NH skin effect whenever $|t_{-l}| \neq |t_l|$ for some l . The β_l values are the roots of the following polynomial

$$t_r \beta^{s+r} + t_{r-1} \beta^{s+r-1} + \dots + (t_0 - E_0) \beta^s + \dots + t_{-s+1} \beta + t_{-s} = 0. \quad (14)$$

If the hopping amplitudes t_l are real, a sufficient condition for the roots of the polynomial to be real and distinct

(so that β_s is real and $|\beta_s|$ is strictly smaller than $|\beta_{s+1}|$) is given by a general theorem of linear algebra [98], requiring some constraints on the hopping amplitudes. Some illustrative examples of NH barrier models displaying real β_s values, without requiring any special symmetry (such as PT symmetry) in the system, are presented in the next section.

A final comment is in order concerning the observability of the NH Hartman effect in an ideal wave packet tunneling experiment. Since we are dealing with a NH barrier, besides scattering states with real energy $E_0 = 2\kappa \cos q$ the heterojunction system of Fig.1(a) could sustain a set of bound (normalizable) states, localized near the barrier region, with complex eigenenergies E_1, E_2, \dots . The energies of such bound states are given by $E_1 = 2\kappa \cos q_1, E_2 = 2\kappa \cos q_2, \dots$, where q_1, q_2, \dots are the poles of the spectral transmission and reflection amplitudes $\mathcal{T}(q), \mathcal{R}(q)$ in the complex q plane with $\text{Im}(q) < 0$. The bound states are unstable if the imaginary part of their energy is positive. In this case, i.e. in presence of unstable states, the Hartman effect could be hard to be observed (or could be observed only transiently), since any noise in the system can secularly amplify the unstable bound states, preventing the observation of the tunneled wave packet. On this issue, see for instance Ref. [99]. We note that, if the energy spectrum of the potential barrier under OBC (i.e. when not attached to the two left and right leads) is real or all energies are stable (i.e. with negative imaginary parts, like in purely dissipative systems), then it is likely that unstable bound states will not arise when we attach the barrier to the left and right Hermitian leads, a result which is exact in the $\kappa \rightarrow 0$ limit. In the following, we will not consider NH barrier potentials that display unstable bound states, or assume that possible unstable bound states have a small imaginary part of the eigenenergy so as not to prevent the observation of wave packet tunneling over a limited temporal window.

4 Illustrative examples and numerical simulations

We illustrate the general results on the NH Hartman effect, presented in the previous section, by considering two prototypical models of NH tight-binding barriers, corresponding to $M = 1$ (the generalized Hatano-Nelson model) and $M = 2$ (the NH Rice-Mele model).

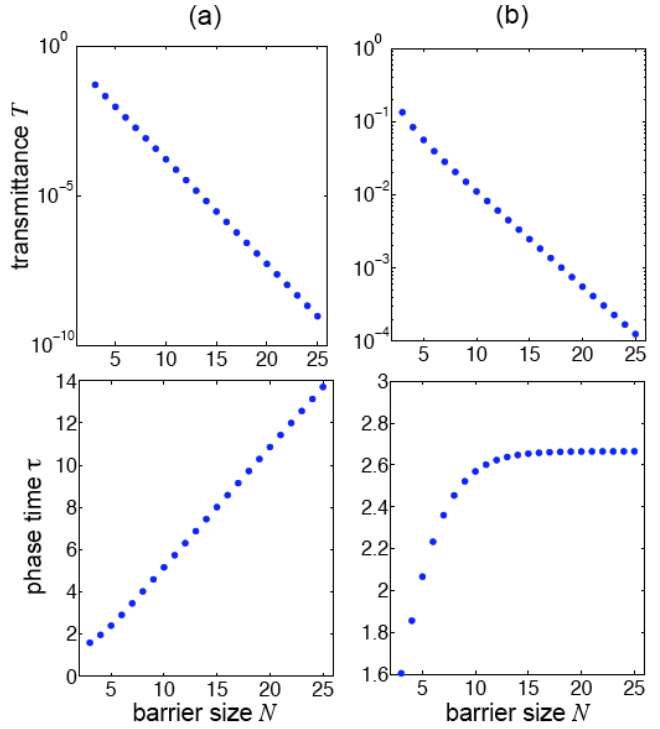


Figure 2 Behavior of the transmittance $T = |\mathcal{T}|^2$ on a log scale (upper panels), and of tunneling phase time τ (lower panels) versus the barrier size N in two different types of NH barriers with nearest-neighbor hopping. (a) A dissipative barrier with complex on-site potential ($\kappa = t_{-1} = t_1 = 1, t_0 = 2.1 - 0.2i$); (b) The NH Hatano-Nelson barrier with non-reciprocal hopping and real on-site potential ($\kappa = t_{-1} = 1, t_0 = 1.85, t_1 = 0.8$). The incident wave has a Bloch wave number $q = \pi/2$, corresponding to the energy $E_0 = 2\kappa \cos q = 0$. Note that the Hartman effect, i.e. the independence of the phase time τ on barrier size in the large N limit, is found in the second model solely.

4.1 The generalized Hatano-Nelson model

Let us assume that the unit cell of the barrier comprises a single site, i.e. $M = 1$, and that we have only nearest-neighbor hopping t_{-1}, t_1 in the lattice ($r = s = 1$), so that $H(\beta) = t_{-1}/\beta + t_0 + t_1\beta$. This corresponds to the clean Hatano-Nelson model [60,84], which does not possess any symmetry. The roots β_1, β_2 to the determinantal equation $H(\beta) - E_0 = 0$ read

$$\beta_{1,2} = \frac{E_0 - t_0}{2t_1} \pm \frac{1}{t_1} \sqrt{\left(\frac{E_0 - t_0}{2}\right)^2 - t_1 t_{-1}} \quad (15)$$

with $E_0 = 2\kappa \cos q$. Then the condition that the phase of $\beta_s = \beta_1$ does not depend on q can be met provided that the β 's roots are real. This excludes the case where the on-site potential t_0 is complex, such as in a barrier

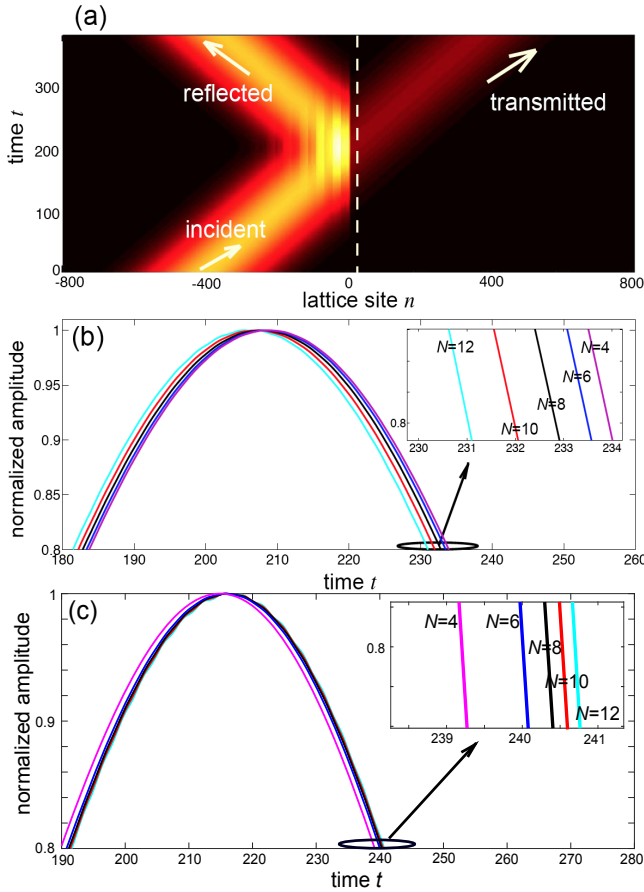


Figure 3 Scattering dynamics at a NH barrier with non-reciprocal nearest neighbor hopping amplitudes [$\kappa = t_{-1} = 1$, $t_0 = 1.85$, $t_1 = 0.8$ as in Fig.2(b)]. (a) Space-time scattering dynamics of an incident Gaussian wave packet for barrier width $N = 6$. The input wave function is $\psi_n(0) = \exp[-(n+400)^2/w_0^2 - iqn]$ with carrier Bloch wave number $q = \pi/2$ and size $w_0 = 150$. (b) Temporal behavior of the wave function amplitude $|\psi_n(t)|$ in the site $n = 20$, after the barrier [indicated by the dashed vertical curve in (a)], normalized to its maximum value, for a few increasing values of the barrier size N ($N = 4, 6, 8, 10, 12$). The barrier is located between $n = 1$ and $n = N$. As shown in the inset, as N increases the rate $\Delta\tau/\Delta N$ of the waveform time advancement $\Delta\tau$ reaches a value close to 0.5, indicating that the tunneling phase time becomes nearly independent of the barrier size N for large N . (c) Same as (b), but for parameter values $\kappa = t_{-1} = t_1 = 1$, $t_0 = 2.1 - 0.2i$ [as in Fig.2(a)]. In this case there is not any advancement of the waveform as the barrier N is increased.

with dissipation. However, when the on-site potential energy t_0 and $t_1 t_{-1}$ are real numbers, the condition for the observation of the NH Hartman effect is satisfied for $(E_0 - t_0)^2/4 - t_1 t_{-1} > 0$. In particular, for an incident wave with zero energy $E_0 = 0$ at the band center, corresponding to a Bloch wave number $q = \pi/2$, the NH Hartman

effect is observed provided that $t_0^2 > 4t_1 t_{-1}$. In this case, in order to avoid the appearance of unstable modes we assume $t_1 t_{-1} > 0$, corresponding to an entirely real energy spectrum of the Hatano-Nelson Hamiltonian under open boundary conditions. As an example, Fig.2 shows the spectral transmittance $T = |\mathcal{F}|^2$ and tunneling phase time τ versus barrier size N , as obtained by numerically solving the matching conditions at the junctions [Eqs.(A.11-A.19) in Appendix A], for an incidence wave with zero energy ($q = \pi/2, E_0 = 0$) in two types of NH barrier models. In the former model [Fig.2(a)] we have a dissipative on-site potential barrier with symmetric hopping amplitudes, which does not display the NH Hartman effect. In the latter case we have a NH barrier with asymmetric hopping amplitudes and real on-site potential [Fig.2(b)], which clearly shows the NH Hartman effect, indicated by the saturation of the tunneling phase time τ as N is increased.

We checked the occurrence of the Hartman effect in the Hatano-Nelson barrier model with non-reciprocal hopping and real on-site potential by direct numerical simulations of the time-dependent Schrödinger equation on the lattice. A spatially-broad Gaussian wave packet with carrier Bloch wave number $q = \pi/2$ is injected to the barrier from the left side, and the peak delay of the transmitted wave packet is detected after the scattering event. Figure 3(a) depicts on a pseudocolor map a typical temporal evolution of the normalized occupation amplitudes $|\psi_n(t)|/\sqrt{\sum_n |\psi_n(t)|^2}$ for a barrier size $N = 6$ and for the same parameter values as in Fig.2(b). The initial wave packet, at time $t = 0$, is well localized on the left side of the barrier with a broad Gaussian distribution of size $w_0 = 150$ (much larger than the barrier width to limit wave packet distortion effects [17, 30]) and carrier Bloch wave number $q = \pi/2$, corresponding to the energy $E_0 = 0$. Figure 3(b) shows the temporal behavior of the wave function amplitude $|\psi_n(t)|$ in the site $n = 20$ after the barrier [indicated by the dashed vertical curve in Fig.3(a)], normalized to its maximum value, for a few increasing values of the barrier size N ($N = 4, 6, 8, 10, 12$). The delay time $\tau_d(N)$ of the transmitted wave packet at the reference site $n = 20$, for a barrier of size N , can be written as $\tau_d(N) = \tau_d^{(1)} + \tau_d^{(2)}$, where $\tau_d^{(1)}$ is the delay time due to the crossing of the barrier and $\tau_d^{(2)}$ is the traversal time in the leads, where the wave packet propagates at the group velocity $v_g = 2\kappa \cos q = 2$. In the presence of the Hartman effect, i.e. independence of $\tau_d^{(1)}$ on barrier size N for large N , as we increase the barrier size N by ΔN , $\tau_d^{(1)}$ does not change while $\tau_d^{(2)}$ clearly decreases by $\Delta N/v_g = \Delta N/2$, since the spatial distance that the wave packet spends in the leads is reduced by ΔN . This means that, indicating by $\Delta\tau = \tau_d(N) - \tau_d(N + \Delta N)$ the time advancement of the

peak of the wave packet, at the reference site $n = 20$, as we increase the barrier width from N to $N + \Delta N$, in the presence of the Hartman effect the ratio $\Delta\tau/\Delta N$ should reach the value $\Delta\tau/\Delta N \approx 1/2$, independent of N . In Fig.3(c) we can clearly see a slight advancement $\Delta\tau$ in time of the peak of the waveform as N is increased, with a rate $\Delta\tau/\Delta N$ that reaches an asymptotic value close to 0.5 as N is increased [see the inset in Fig.3(b)], which is thus a signature of the independence of tunneling phase time on barrier width. For parameter values where the phase of $\beta_s(q)$ does not show any stationary point, for example in the dissipative barrier of Fig.2(a), there is not any advancement of the waveform as N is increased [see Fig.3(c)], indicating the absence of the Hartman effect.

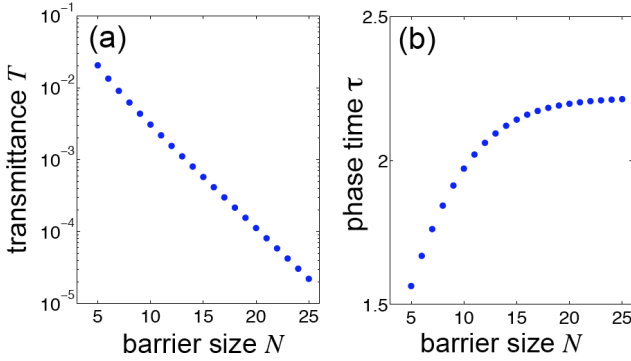


Figure 4 Behavior of the transmittance $T = |\mathcal{T}|^2$ on a log scale (a) and tunneling phase time τ (b) versus the barrier size N in the NH generalized Hatano-Nelson barrier with nearest and next-to-nearest hopping amplitudes $\kappa = 1$, $t_{-2} = 0.275$, $t_{-1} = -0.8667$, $t_0 = -2.3627$, $t_1 = -0.9184$ and $t_2 = 0.25$. The incident wave has a Bloch wave number $q = \pi/2$, corresponding to the energy $E_0 = 2\kappa \cos q = 0$.

In the Hatano-Nelson model with only nearest-neighbor non-reciprocal hopping the tunneling dynamics, and thus the Hartman effect, can be basically reduced to the one of an Hermitian barrier with on-site potential t_0 and effective nearest-neighbor reciprocal coupling $\sqrt{t_1 t_{-1}}$. This can be readily proven after a non-unitary gauge transformation of the wave function ψ_n , which makes the hopping reciprocal in the barrier region (see for instance [63, 93]). This is possible because the generalized Brillouin zone in the Hatano-Nelson model is a circle, i.e. the imaginary part of the Bloch wave number k is homogeneous. However, for long-range non-reciprocal hopping the generalized Brillouin zone is not anymore a circle [63, 66, 69], and the tunneling dynamics cannot

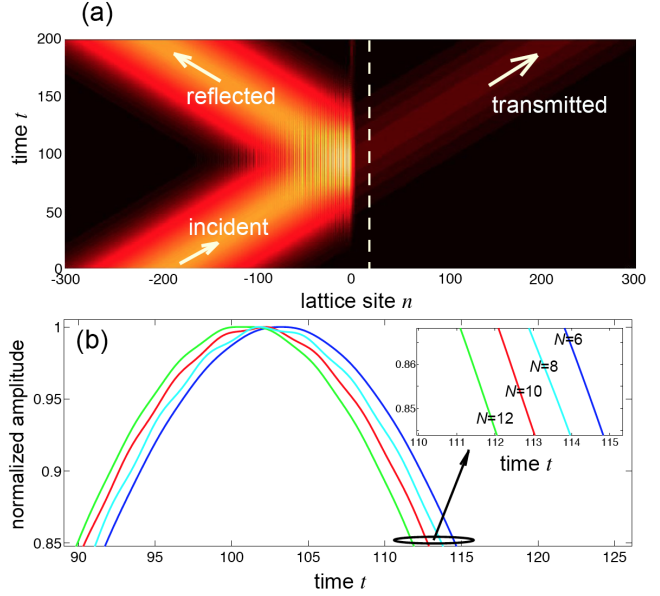


Figure 5 Scattering dynamics at a NH barrier with nearest and next-to-nearest neighbor hopping amplitudes ($\kappa = 1$, $t_{-2} = 0.275$, $t_{-1} = -0.8667$, $t_0 = -2.3627$, $t_1 = -0.9184$ and $t_2 = 0.25$). (a) Space-time scattering dynamics of an incident Gaussian wave packet for barrier width $N = 6$. The input wave function is $\psi_n(0) = \exp[-(n + 190)^2/w_0^2 - iqn]$ with carrier Bloch wave number $q = \pi/2$ and size $w_0 = 80$. (b) Temporal behavior of the wave function amplitude $|\psi_n(t)|$ in the site $n = 20$, after the barrier [indicated by the dashed vertical curve in (a)], for a few increasing values of the barrier size N ($N = 6, 8, 10, 12$). The barrier is located between $n = 1$ and $n = N$. As shown in the inset, for increasing N a waveform temporal advancement is observed, with a rate $\Delta\tau/\Delta N$ of temporal advancement $\Delta\tau$ which asymptotically reaches a value close to 0.5, indicating that the phase time becomes almost independent of barrier width.

be anymore reduced to the one of an Hermitian barrier. For example, the NH Hartman effect can be observed by generalizing the Hatano-Nelson model including next-to-nearest hopping amplitudes, corresponding to $M = 1$ and $s = r = 2$. As an illustrative example, let us consider the NH barrier corresponding to the hopping amplitudes $t_{-2} = 0.275$, $t_{-1} = -0.8667$, $t_0 = -2.3627$, $t_1 = -0.9184$ and $t_2 = 0.25$. For such parameter values, the energy spectrum of the Hamiltonian in the barrier region under open boundaries, i.e. when isolated from the two leads, is entirely real. For an incident wave with an energy E_0 close to zero ($q \approx \pi/2$, $E_0 \approx 0$), the four roots β_i of the determinantal equation $H(\beta) - E_0 = 0$ are real, with $\beta_s = \beta_2 \sim 0.85$. Figure 4 shows the spectral transmittance $T = |\mathcal{T}|^2$ and tunneling phase time τ versus barrier size N , as obtained by numerically solving the matching conditions at the junc-

tions [Eqs.(A.11-A.19) in Appendix A], for an incidence wave with zero energy ($q = \pi/2, E_0 = 0$), clearly indicating the existence of the NH Hartman effect. The scattering dynamics of a spatially-broad Gaussian wave packet across the NH barriers, for a few increasing values of the N , is shown in Fig.5. The rate $\Delta\tau/\Delta N$ of temporal advancement of the wave amplitudes as N is increased, shown in Fig.5(b), becomes close to 0.5 as N is increased, which is a clear signature of the NH Hartman effect.

In the above examples, to observe the Hartman effect the on-site potential energy t_0 has been assumed to be real. For real values of the hopping amplitudes, this ensures that the root $\beta_s(q)$ can be real over a wide range of the Bloch wave number q , leading to the Hartman effect. A natural and interesting question is whether the Hartman effect could be observed for a on-site potential energy t_0 with a non-vanishing imaginary part, for example for $\text{Im}(t_0) < 0$ corresponding to a dissipative on-site potential energy. In this case, stationarity of the phase of $\beta_s(q)$ cannot be anymore realized over a wide range of the Bloch wave number q , however it can occur at isolated values of q . This means that, for a NH barrier with dissipative on-site energy, the Hartman effect can be rather generally observed only for isolated energies of the incoming wave. For example, for a NH barrier with $r = s = 2$ and for parameter values $t_{-1} = t_1 = \kappa = 1$, $t_{-2} = 0.4$, $t_2 = 0.3$ and $t_0 = 1 - 5 - 0.3i$ the phase $\varphi_{\beta_s}(q)$ of $\beta_s(q)$ shows an isolated stationary point at $q = q_0 \simeq 1.7$, so that the Hartman effect should be observable only for an incoming wave with energy $E = 2\kappa \cos q_0 \simeq -0.13$.

4.2 The non-Hermitian Rice-Mele model

As a second illustrative model, we consider a NH extension of the Rice-Mele model [100–104], which is a dimeric lattice corresponding to $M = 2$ sites ($A_1 = A$ and $A_2 = B$) in each unit cell. A schematic of the Rice-Mele model is shown in Fig.6(a). The 2×2 Bloch Hamiltonian $H(\beta)$ for this model reads

$$H(\beta) = \begin{pmatrix} \Delta_A & t_1 + \rho_2/\beta \\ t_2 + \rho_1\beta & \Delta_B \end{pmatrix} \quad (16)$$

where Δ_A, Δ_B are the (generally complex) on-site potential energies in the two sublattices A and B, respectively, $t_{1,2}$ are the left/right intradimer hopping amplitudes and $\rho_{1,2}$ are the left/right interdimer hopping amplitudes. We note that, for $\Delta_A = \Delta_B = 0$, this model reduces to the NH extension of the Su-Schrieffer-Heeger (SSH) model with chiral symmetry, studied in recent works in the context

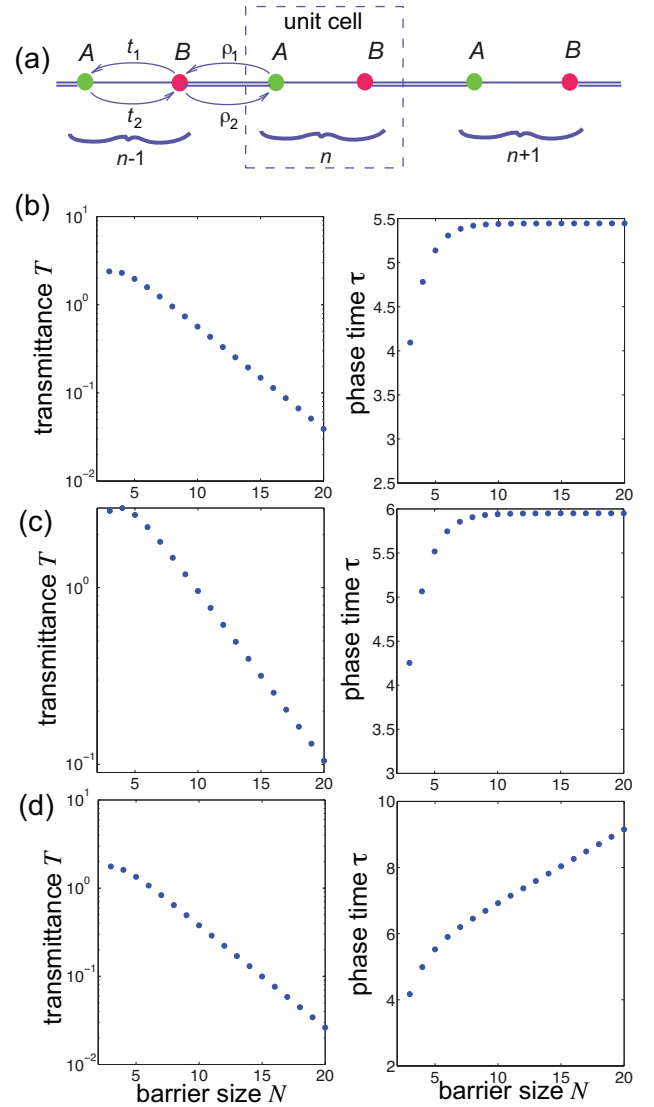


Figure 6 (a) Schematic of the NH Rice-Mele superlattice. The onsite potentials in sublattices A and B are Δ_A and Δ_B , respectively, while the left/right intra-dimer and inter-dimer hopping amplitudes are $t_{1,2}$ and $\rho_{1,2}$, respectively. (b-d) Behavior of the transmittance $T = |\mathcal{T}|^2$ on a log scale (left panels) and tunneling phase time τ (right panels) versus the barrier size N in the NH Rice-Mele barrier for parameter values $\kappa = 1$, $t_1 = 0.8$, $t_2 = 1$, $\rho_1 = 0.5$, $\rho_2 = 0.7$ and for a few different values of the on-site potentials: (b) $\Delta_A = \Delta_B = 0$; (c) $\Delta_A = 0.1i$, $\Delta_B = -0.1i$; (d) $\Delta_A = 0$, $\Delta_B = -0.1i$.

of the NH skin effect and bulk-edge correspondence (see e.g. [63]), while for reciprocal couplings $t_1 = t_2$, $\rho_1 = \rho_2$ and complex on-site potential energies $\Delta_{A,B} = \pm i\delta$, this model reduces to the PT-symmetric SSH model [105]. In both cases we consider parameter values such that, under

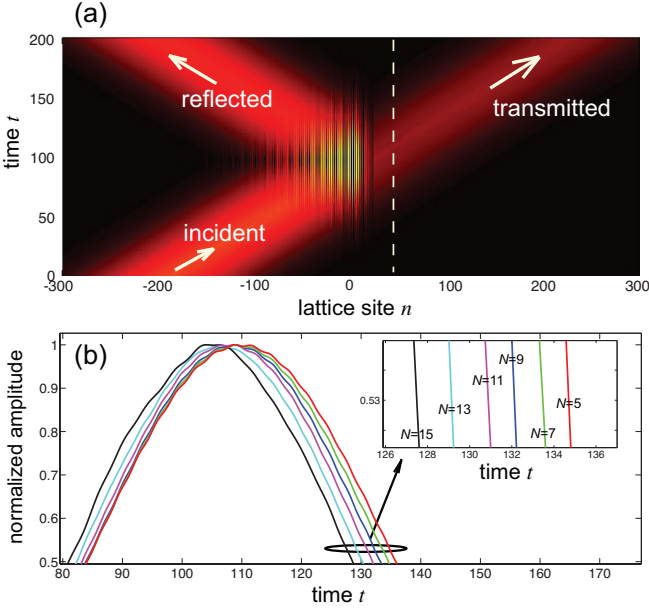


Figure 7 Scattering dynamics at a NH Rice-Mele barrier for parameter values $\kappa = 1$, $t_1 = 0.8$, $t_2 = 1$, $\rho_1 = 0.5$, $\rho_2 = 0.7$, and $\Delta_A = \Delta_B = 0$. (a) Space-time scattering dynamics of an incident Gaussian wave packet for a barrier width $N = 13$. The input wave function is $\psi_n(0) = \exp[-(n+190)^2/w_0^2 - iq_n]$ with carrier Bloch wave number $q = \pi/2$ and size $w_0 = 80$. (b) Temporal behavior of the wave function amplitude $|\psi_n(t)|$ in the site $n = 40$, after the barrier [indicated by the dashed vertical curve in (a)], normalized to its maximum value, for a few increasing values of the barrier size N ($N = 5, 7, 9, 11, 13, 15$). The barrier is located between $n = 1$ and $n = N$. As shown in the inset, an increase $\Delta N = 2$ in the barrier width N (unit cell) corresponds to an advancement in time $\Delta \tau$ of ~ 2 for large N , indicating that the tunneling phase time is nearly independent of the barrier size N .

$$\mathcal{M} = \begin{pmatrix} -\kappa \exp(iq) & \kappa(t_1\beta_1 + \rho_2) & \kappa(t_1\beta_2 + \rho_2) & 0 \\ -\kappa & \rho_2(E_0 - \Delta_A) & \rho_2(E_0 - \Delta_A) & 0 \\ 0 & \rho_1\beta_1^N(t_1\beta_1 + \rho_2) & \rho_1\beta_2^N(t_1\beta_2 + \rho_2) & -\kappa \\ 0 & \kappa(E_0 - \Delta_A)\beta_1^N & \kappa(E_0 - \Delta_A)\beta_2^N & -\kappa \exp(iq) \end{pmatrix}. \quad (24)$$

According to the general result shown in Sec.3, the NH Hartman effect is observed provided that the phase of the root $\beta_s = \beta_1$ to Eq.(17) does not depend on q . This condition can be satisfied when the intra- and inter-dimer hopping amplitudes $t_{1,2}$, $\rho_{1,2}$ are real and the on-site potential energies are either real or satisfy the condition $\Delta_A = \Delta_B^*$, which basically corresponds PT symmetry in the system. Hence, like in continuous models of the NH Hartman effect [49, 50], PT symmetry ensures the inde-

pendence of the tunneling phase time on barrier width for long barriers. However, the NH Hartman effect can be observed even without any complex on-site potential, for example by assuming $\Delta_A = \Delta_B = 0$, as a result of non-reciprocal hopping in the lattice. Figure 6(b-d) shows an example of numerically-computed spectral transmittance and tunneling phase time in a NH Rice-Mele barrier versus barrier size N for an incoming wave with Bloch wave number $q_0 = \pi/2$, illustrating different tunneling regimes.

$$t_1\rho_1\beta^2 + [t_1t_2 + \rho_1\rho_2 - (E_0 - \Delta_A)(E_0 - \Delta_B)]\beta + \rho_2t_2 = 0 \quad (17)$$

while the eigenvectors $U^{(1,2)}$ read

$$U^{(1)} = \begin{pmatrix} t_1 + \rho_2/\beta_1 \\ E - \Delta_A \end{pmatrix}, \quad U^{(2)} = \begin{pmatrix} t_1 + \rho_2/\beta_2 \\ E - \Delta_A \end{pmatrix}. \quad (18)$$

The spectral reflection and transmission amplitudes $\mathcal{R}(q)$ and $\mathcal{T}(q)$ are obtained by imposing the matching conditions of the scattering solution at the junctions, i.e. by imposing the following equations

$$E_0\psi_0 = \kappa\psi_{-1} + \kappa\psi_1^{(A)} \quad (19)$$

$$E_0\psi_1^{(A)} = \Delta_A\psi_1^{(A)} + \kappa\psi_0 + t_1\psi_1^{(B)} \quad (20)$$

$$E_0\psi_N^{(B)} = \Delta_B\psi_N^{(B)} + \kappa\psi_{N+1} + t_2\psi_N^{(A)} \quad (21)$$

$$E_0\psi_{N+1} = \kappa\psi_{N+2} + \kappa\psi_N^{(B)}. \quad (22)$$

This yields the following linear inhomogeneous system in the variables $\mathcal{R}(q)$, G_1 , G_2 and $\mathcal{T}(q)$

$$\mathcal{M} \begin{pmatrix} \mathcal{R}(q) \\ G_1 \\ G_2 \\ \mathcal{T}(q) \end{pmatrix} = \begin{pmatrix} E_0 - \kappa \exp(iq) \\ \kappa \\ 0 \\ 0 \end{pmatrix} \quad (23)$$

with matrix \mathcal{M} given by

In particular, note that the Hartman effect is observed in Figs.6(b) and (c), where the condition $\Delta_A = \Delta_B^*$ is satisfied, but not in Fig.6(d). The scattering dynamics of a spatially-broad Gaussian wave packet across the NH barrier, showing the Hartman effect and corresponding to parameter values of Fig.6(b), is shown in Fig.7. Figure 7(a) depicts a typical space-time map of wave packet scattering for a barrier comprising $N = 13$ unit cells, while Fig.7(b) shows the temporal behavior of normalized waveforms observed beyond the barrier at a given lattice site ($n = 40$) and for a few increasing values of N . Note that the rate $\Delta\tau/\Delta N$ of temporal advancement $\Delta\tau$ of the wave amplitudes, as N is increased, reaches an asymptotic value close to 1, as clearly visible in the inset of Fig.7(b). This is a clear indication of the saturation of the tunneling phase time for increasing values of N , i.e. of the Hartman effect.

5 Conclusion.

In this work we investigated wave scattering from a non-Hermitian potential barrier in the tight-binding picture, and derived a rather general condition for the existence of the Hartman effect, i.e. the independence of the phase tunneling time on barrier width. Our results extend to non-Hermitian systems on a lattice the rather paradoxical effect of wave tunneling in Hermitian systems, indicating that the Hartman effect in non-conservative systems can be observed without any special symmetry requirement, such as PT symmetry. The appearance of the NH Hartman effect has been illustrated by considering tunneling across NH barriers described by the generalized Hatano-Nelson model and by a NH extension of the Rice-Mele model.

A Matching conditions and scattering analysis

In this Appendix we provide the detailed form of the scattering wave equations, obtained from the matching conditions at the junctions, in the special case where we have a single site in each unit cell of the barrier, i.e. for $M = 1$. The more general case $M \geq 2$ can be handled in a similar way, as an explicit example is given in Sec. 4.2 of the main text. For $M = 1$, the Hamiltonian $H(\beta)$ of the barrier superlattice is a scalar and given by the Laurent polynomial

$$H(\beta) = \frac{t_{-s}}{\beta^s} + \frac{t_{-s+1}}{\beta^{s-1}} + \dots + t_0 + t_1\beta + \dots + t_r\beta^r \quad (\text{A.1})$$

where $t_{\mp l}$ are the left or right hopping amplitudes among sites distant $|l|$ in the lattice and $s, r \geq 1$ are the largest orders of left (s) or right (r) hopping. We recall that, for non-reciprocal couplings, owing to the NH skin effect the energy spectrum of the NH superlattice with Hamiltonian $H(\beta)$ strongly depends on the boundary conditions [63, 66, 69, 73, 75, 97]. In particular, the PBC energy spectrum E_{PBC} is a closed loop \mathcal{C}_1 in complex energy plane, which is defined by the relation $E_{PBC} = H(\beta = \exp(ik))$ with k real. In other words, the E_{PBC} energy spectrum is the image of the unit circle $|\beta| = 1$ in complex β plane (Brillouin zone). On the other hand, the energy spectrum E_{OBC} under OBC is defined by the set of energies E such that $|\beta_s| = |\beta_{s+1}|$, where β_l ($l = 1, 2, 3, \dots, r + s$) are the $(r + s)$ roots of the polynomial (determinantal equation) $\beta^s H(\beta) - E_0 \beta^s = 0$, ordered according to Eq.(3) [69, 73, 75, 97]. In a NH system displaying the NH skin effect, the energy spectrum E_{OBC} differs from E_{PBC} and describes one (or a set of) open arc internal to the PBC energy spectrum loop \mathcal{C}_1 . The loci of $|\beta_s| = |\beta_{s+1}|$ in complex β plane defines the generalized Brillouin zone, which is not the unit circle as a signature of the NH skin effect.

For the scattering problem of the superlattice barrier attached to the two Hermitian tight-binding leads, for an incoming wave with wave number q and energy $E_0 = 2\kappa \cos q$, incident on the left side of the barrier, the scattering eigenfunction of the system at energy E_0 reads can be searched in the form

$$\psi_n = \begin{cases} \exp(-iqn) + \mathcal{R}(q) \exp(iqn) & n \leq 0 \\ \sum_{l=1}^{s+r} G_l \beta_l^n & 1 \leq n \leq N \\ \mathcal{T}(q) \exp[-iq(n - N - 1)] & n \geq N + 1 \end{cases} \quad (\text{A.2})$$

where $\beta_1, \beta_2, \dots, \beta_{s+r}$ are the $(r + s)$ roots of the polynomial (determinantal equation) $\beta^s H(\beta) - E_0 \beta^s = 0$, ordered according to Eq.(3). The matching conditions at the junctions are obtained by imposing that the Ansatz (A.2) satisfies

the stationary Schrödinger equation at the lattice sites $n = 0, 1, 2, \dots, s$ and $n = N - r + 1, N - r + 2, \dots, N, N + 1$, i.e.

$$E_0\psi_0 = \kappa(\psi_{-1} + \psi_1) \quad (\text{A.3})$$

$$(E_0 - t_0)\psi_1 = \kappa\psi_0 + t_1\psi_2 + t_2\psi_3 + \dots + t_r\psi_{r+1} \quad (\text{A.4})$$

$$(E_0 - t_0)\psi_2 = t_{-1}\psi_1 + t_1\psi_3 + t_2\psi_4 + \dots + t_r\psi_{r+2} \quad (\text{A.5})$$

... ..

$$(E_0 - t_0)\psi_s = t_{-s+1}\psi_1 + t_{-s+2}\psi_2 + \dots + t_r\psi_{r+s} \quad (\text{A.6})$$

$$(E_0 - t_0)\psi_{N-r+1} = t_{-s}\psi_{N-r-s+1} + t_{-s+1}\psi_{N-r-s+2} + t_{r-1}\psi_N \quad (\text{A.7})$$

... ..

$$(E_0 - t_0)\psi_{N-1} = t_{-s}\psi_{N-s-1} + t_{-s+1}\psi_{N-s} + \dots + t_{-1}\psi_{N-2} + t_1\psi_N \quad (\text{A.8})$$

$$(E_0 - t_0)\psi_N = t_{-s}\psi_{N-s} + t_{-s+1}\psi_{N-s+1} + \dots + t_{-1}\psi_{N-1} + \kappa\psi_{N+1} \quad (\text{A.9})$$

$$E_0\psi_{N+1} = \kappa\psi_{N+2} + \kappa\psi_N. \quad (\text{A.10})$$

where we assumed $N > (r + s)$. This yields the following set of $(s + r + 2)$ linear inhomogeneous equations

$$E_0[1 + \mathcal{R}(q)] = \kappa[\exp(iq) + \mathcal{R}(q)\exp(-iq)] + \kappa \sum_{l=1}^{r+s} G_l \beta_l \quad (\text{A.11})$$

$$(E_0 - t_0) \sum_{l=1}^{r+s} G_l \beta_l = \kappa[1 + \mathcal{R}(q)] + t_1 \sum_{l=1}^{r+s} G_l \beta_l^2 + t_2 \sum_{l=1}^{r+s} G_l \beta_l^3 + \dots + t_r \sum_{l=1}^{r+s} G_l \beta_l^{r+1} \quad (\text{A.12})$$

$$(E_0 - t_0) \sum_{l=1}^{r+s} G_l \beta_l^2 = t_{-1} \sum_{l=1}^{r+s} G_l \beta_l + t_1 \sum_{l=1}^{r+s} G_l \beta_l^3 + t_2 \sum_{l=1}^{r+s} G_l \beta_l^4 + \dots + t_r \sum_{l=1}^{r+s} G_l \beta_l^{r+2} \quad (\text{A.13})$$

... ..

$$(E_0 - t_0) \sum_{l=1}^{r+s} G_l \beta_l^s = t_{-s+1} \sum_{l=1}^{r+s} G_l \beta_l + t_{-s+2} \sum_{l=1}^{r+s} G_l \beta_l^2 + \dots + t_r \sum_{l=1}^{r+s} G_l \beta_l^{s+r} \quad (\text{A.14})$$

$$(E_0 - t_0) \sum_{l=1}^{r+s} G_l \beta_l^{N-r+1} = t_{-s} \sum_{l=1}^{r+s} G_l \beta_l^{N-s-r+1} + t_{-s+1} \sum_{l=1}^{r+s} G_l \beta_l^{N-r-s+2} + \dots + t_{r-1} \sum_{l=1}^{r+s} G_l \beta_l^N \quad (\text{A.15})$$

... ..

$$(E_0 - t_0) \sum_{l=1}^{r+s} G_l \beta_l^{N-1} = t_{-s} \sum_{l=1}^{r+s} G_l \beta_l^{N-s-1} + t_{-s+1} \sum_{l=1}^{r+s} G_l \beta_l^{N-s} + \dots + t_1 \sum_{l=1}^{r+s} G_l \beta_l^N \quad (\text{A.17})$$

$$(E_0 - t_0) \sum_{l=1}^{r+s} G_l \beta_l^N = t_{-s} \sum_{l=1}^{r+s} G_l \beta_l^{N-s} + t_{-s+1} \sum_{l=1}^{r+s} G_l \beta_l^{N-s+1} + \dots + t_{-1} \sum_{l=1}^{r+s} G_l \beta_l^{N-1} + \kappa \mathcal{T}(q) \quad (\text{A.18})$$

$$E_0 \mathcal{T}(q) = \kappa \mathcal{T}(q) \exp(-iq) + \kappa \sum_{l=1}^{r+s} G_l \beta_l^N, \quad (\text{A.19})$$

which can be solved to determine the amplitudes G_1, G_2, \dots, G_{s+r} of evanescent waves in the barrier region, and the spectral transmission and reflection coefficients $\mathcal{T}(q)$ and $\mathcal{R}(q)$ for a given value of the Bloch wave number q , i.e. energy $E_0 = 2\kappa \cos q$ of the incoming wave.

B Asymptotic form of the spectral transmission amplitude

In this Appendix we prove that the spectral amplitude $\mathcal{T}(q)$, in the limit of a long barrier (i.e. in the large N limit), takes the form

$$\mathcal{T}(q) = \tilde{\mathcal{T}}(q) \beta_s^N \quad (\text{B.1})$$

where $\tilde{\mathcal{F}}(q)$ is independent of N . This result holds provided that the condition $|\beta_s| < |\beta_{s+1}|$ is strictly satisfied, i.e. that the energy E_0 of the incoming wave does not belong to the energy spectrum E_{OBC} of the superlattice under OBC. To prove this statement, we should solve the inhomogeneous linear system of $(s+r+2)$ equations, obtained from the matching conditions at the junctions (see e.g. Eqs.(A.11-A.19) in Appendix A), for the unknown variables $G_1, G_2, \dots, G_{l+s}, \mathcal{R}(q), \mathcal{T}(q)$ in the large N limit. Since the coefficients of the linear system contain powers of $\sim \beta_l^N$, to provide an asymptotic solution to the system in the large N limit it is worth rewriting the equations after suitable scaling of the variables G_l and $\mathcal{T}(q)$, so as the order of magnitude of coefficients in the resulting equations can be readily visualized in the large N limit. Such a scaling analysis is similar to the one used in NH lattices displaying the NH skin effect to compute the generalized Brillouin zone (see for instance [69, 75, 97]). Specifically, let us introduce the following substitutions

$$G_l = g_l \text{ for } l = 1, 2, \dots, s, \quad G_l = g_l \left(\frac{\beta_s}{\beta_l} \right)^N \text{ for } l = s+1, s+2, \dots, s+r, \quad \mathcal{T}(q) = \tilde{\mathcal{T}}(q) \beta_s^N \quad (\text{B.2})$$

and let us assume that the inequality $|\beta_s| < |\beta_{s+1}|$ is strictly satisfied. In this way, it can be readily shown that in the first $(s+1)$ equations in the system [e.g. Eqs.(A.11-A.14) in Appendix A] the coefficients of the amplitudes $g_{s+1}, g_{s+2}, \dots, g_{s+r}$ vanish in the large N limit, since they are expressed in terms of powers $\sim (\beta_s/\beta_l)^N$ and $|\beta_l| > \beta_s$ ($l = s+1, s+2, \dots, s+r$). Therefore, in the large N limit the first set of $(s+1)$ equations of the system are decoupled from the other ones and can be solved, providing the solution to $\mathcal{R}(q), g_1, g_2, \dots, g_s$ which are independent of N . The other $(r+1)$ equations of the system [e.g. Eqs.(A.15-A.19)] of Appendix A] can be then solved to determine the amplitudes $g_{s+1}, g_{s+2}, \dots, g_{s+r}$ and $\tilde{\mathcal{T}}(q)$. To this aim, it is worth dividing both sides of such set of equations by β^s . In this way, in the large N limit the coefficients of the amplitudes g_l , with $l < s$, are vanishing while all other coefficients of g_l and $\tilde{\mathcal{T}}(q)$ are independent of N . Therefore, the resulting solution to $\tilde{\mathcal{T}}(q)$ is independent of N . This proves the main result stated by Eq.(B1).

Disclosures. The author declares no conflicts of interest.

Acknowledgment. The author acknowledges the Spanish State Research Agency, through the Severo-Ochoa and Maria de Maeztu Program for Centers and Units of Excellence in R&D (Grant No. MDM-2017-0711).

Data Availability. No data were generated or analyzed in the presented research.

Key words. Non-Hermitian physics, Tunneling, Traversal Time, non-Hermitian lattices

References

- [1] E. Merzbacher, *Phys. Today* **2002**, 55, 44.
- [2] E. P. Wigner, *Phys. Rev.* **1955**, 98, 145.
- [3] T. E. Hartman, *J. Appl. Phys.* **1962**, 33, 3427.
- [4] M. Büttiker, R. Landauer, *Phys. Rev. Lett.* **1982**, 49, 1739.
- [5] M. Büttiker, *Phys. Rev. B* **1983**, 27, 6178.
- [6] R. Landauer, *Nature* **1989**, 341, 567.
- [7] E. H. Hauge, J. A. Støvneng, *Rev. Mod. Phys.* **1989**, 61, 917.
- [8] Th. Martin, R. Landauer, *Phys. Rev. A* **1992**, 45, 2611.
- [9] V.S. Olkhovsky, E. Recami, *Phys. Rep.* **1992**, 214, 339.
- [10] R. Landauer, T. Martin, *Rev. Mod. Phys.* **1994**, 66, 217.
- [11] A.M. Steinberg, *Phys. Rev. Lett.* **1995**, 74, 2405.
- [12] V.S. Olkhovsky, E. Recami, F. Raciti, A.K. Zaichenko, *J. Phy. I* **1995**, 5, 1351.
- [13] R.Y. Chiao, A.M. Steinberg, *Progress in Optics* **1997**, 37, 345.
- [14] G. Nimtz, W. Heitmann, *Prog. Quantum Electron.* **1997**, 21, 81.
- [15] H.G. Winful, *Nature* **2003**, 424, 638.
- [16] V. S. Olkhovsky, E. Recami, J. Jakiel, *Phys. Rep.* **2004**, 398, 133.
- [17] H.G. Winful, *Phys. Rep.* **2006**, 436, 1.
- [18] M. Hasan, B.P. Mandal, *EPL* **2021**, 133, 20001.
- [19] A.S. Landsman, M. Weger, J. Maurer, R. Boge, A. Ludwig, S. Heuser, C. Cirelli, L. Gallmann, U. Keller, *Optica* **2014**, 1, 343.
- [20] U. Satya Sainadh, R.T. Sang, I.V. Litvinyuk, *J. Phys. Photonics.* **2020**, 2, 042002.
- [21] D. Sokolovski, E. Akhmatskaya, *Sci. Rep.* **2021**, 11, 10040.
- [22] D. Sokolovski, E. Akhmatskaya, *EPL* **2021**, 136, 20001.
- [23] A. Ranfagni, D. Mugnai, D., P. Fabeni, G.P. Pazzi, *Appl. Phys. Lett.* **1991**, 58, 774.
- [24] A. Enders, G. Nimtz, *J. Phys. I* **1992**, 2, 1693.
- [25] A.M. Steinberg, P.G. Kwiat, R. Chiao, *Phys. Rev. Lett.* **1993**, 71, 708.
- [26] C. Spielmann, R. Szipocs, A. Stingl, F. Krausz, *Phys. Rev. Lett.* **1994**, 73, 2308.
- [27] Ph. Balcou, L. Dutriaux, *Phys. Rev. Lett.* **1997**, 78, 851.
- [28] S. Longhi, M. Marano, P. Laporta, M. Belmonte, *Phys. Rev. E* **2001**, 64, 055602.
- [29] S. Longhi, P. Laporta, M. Belmonte, E. Recami, *Phys. Rev. E* **2002**, 65, 046610.

- [30] S. Longhi, M. Marano, M. Belmonte, P. Laporta, *IEEE J. Sel. Topics Quantum Electron.* **2003**, 9, 4.
- [31] P. Eckle, A.N. Pfeiffer, C. Cirelli, A. Staudte, R. Dörner, H.G. Muller, M. Büttiker, U. Keller, *Science* **2008**, 322, 1525.
- [32] L. Torlina, F. Morales, J. Kaushal, I. Ivanov, A. Kheifets, A. Zielinski, A. Scrinzi, H. G. Muller, S. Sukiasyan, M. Ivanov, O. Smirnova, *Nat. Phys.* **2015**, 11, 503.
- [33] N. Camus, E. Yakaboylu, L. Fechner, M. Klaiber, M. Laux, Y. Mi, K.Z. Hatsagortsyan, T. Pfeifer, C.H. Keitel, R. Moshhammer, *Phys. Rev. Lett.* **2017**, 119, 023201.
- [34] U. S. Sainadh, H. Xu, X. Wang, A. Atia-Tul-Noor, W. C. Wallace, N. Douguet, A. Bray, I. Ivanov, K. Bartschat, A. Kheifets, R. T. Sang, I. V. Litvinyuk, *Nature* **2019**, 568, 75.
- [35] R. Ramos, D. Spierings, I. Racicot, A.M. Steinberg, *Nature* **2020**, 583, 529.
- [36] D.C. Spierings, A.M. Steinberg, *Phys. Rev. Lett.* **2021**, 127, 133001.
- [37] F. Badshah, G.-Q. Ge, M. Irfan, S. Qamar, S. Qamar, *Sci. Rep.* **2018**, 8, 1864.
- [38] R.A. Sepkhanov, M.V. Medvedyeva, C.W.J. Beenakker, *Phys. Rev. B* **2009**, 80, 245433.
- [39] Z. Wu, K. Chang, J.T. Liu, X.J. Li, K.S. Chan, *J. Appl. Phys.* **2009**, 105, 043702
- [40] F. Sattari and E. Faizabadi, *AIP Advances* **2012**, 2, 012123.
- [41] F. Sattari and E. Faizabadi, *Sci. Rep.* **2021**, 11, 17617.
- [42] J. Tepper, J. Barnas, *J. Phys.: Condens. Matter* **2019**, 31, 225302.
- [43] R.S. Dumont, T. Rivlin, E. Pollak, *New J. Phys.* **2020**, 22, 093060.
- [44] F. Raciti, G. Salesi, *J. Phys. I* **1994**, 4, 1783.
- [45] G. Nimtz, H. Spieker, H.M. Brodowsky *J. Phys. I* **1994**, 4, 1379.
- [46] P. Angeopoulos, S. Baskoutas, A. Jannussis, R. Mignani, V. Papatheou, *Int. J. Mod. Phys. B* **1993**, 9, 2083.
- [47] F. Delgado, G. Muga, A. Rushhaupt, *Phys Rev A* **2004**, 69, 022106.
- [48] A. Paul, A. Saha, S. Bandopadhyay, B. Dutta-Roy, *Eur. Phys. J. D* **2007**, 42, 495.
- [49] M. Hasan, B.P. Mandal, *Eur. Phys. J. Plus* **2020**, 135, 84.
- [50] M. Hasan, V.N. Singh, B.P. Mandal, *Eur. Phys. J. Plus* **2020**, 135, 640.
- [51] Y. Ashida, Z. Gong, M. Ueda, *Advances in Physics* **2020**, 69, 3.
- [52] L. Feng, R. El-Ganainy, L. Ge, *Nat. Photonics* **2017**, 11, 752.
- [53] R. El-Ganainy, K. G. Makris, M. Khajavikhan, Z. H. Musslimani, S. Rotter, D. N. Christodoulides, *Nat. Phys.* **2018**, 14, 11.
- [54] S. Longhi, *EPL* **2017**, 120, 64001.
- [55] M.-A. Miri, A. Alú, *Science* **2019**, 363, eaar7709.
- [56] S. K. Ozdemir, S. Rotter, F. Nori, L. Yang, *Nat. Mater.* **2019**, 18, 783.
- [57] C. M. Bender, S. Boettcher, *Phys. Rev. Lett.* **1998**, 80, 5243.
- [58] C. M. Bender, *Rep. Prog. Phys.* **2007**, 70, 947.
- [59] D. Leykam, K. Y. Bliokh, C. Huang, Y. D. Chong, F. Nori, *Phys. Rev. Lett.* **2017**, 118, 040401.
- [60] Z. Gong, Y. Ashida, K. Kawabata, K. Takasan, S. Higashikawa, M. Ueda, *Phys. Rev. X* **2018**, 8, 031079.
- [61] H. Shen, B. Zhen, L. Fu, *Phys. Rev. Lett.* **2018**, 120, 146402.
- [62] F.K. Kunst, E. Edvardsson, J.C. Budich, E.J. Bergholtz, *Phys. Rev. Lett.* **2018**, 121, 026808.
- [63] S. Yao, Z. Wang, *Phys. Rev. Lett.* **2018**, 121, 086803.
- [64] V. M. Martinez Alvarez, J. E. Barrios Vargas, L. E. F. Foa Torres, *Phys. Rev. B* **2018**, 97, 121401.
- [65] S. Yao, F. Song, Z. Wang, *Phys. Rev. Lett.* **2018**, 121, 136802.
- [66] C.H. Lee, R. Thomale, *Phys. Rev. B* **2019**, 99, 201103.
- [67] H. Zhou, J.Y. Lee, *Phys. Rev. B* **2019**, 99, 235112.
- [68] C.-H. Liu, H. Jiang, S. Chen, *Phys. Rev. B* **2019**, 125103.
- [69] K. Yokomizo, S. Murakami, *Phys. Rev. Lett.* **2019**, 123, 066404.
- [70] A. Ghatak, T. Das, *J. Phys.: Condens. Matter* **2019**, 31, 263001.
- [71] K. Kawabata, K. Shiozaki, M. Ueda, M. Sato, *Phys. Rev. X*, **2019**, 9, 041015.
- [72] S. Longhi, *Phys. Rev. Research* **2019**, 1, 023013.
- [73] N. Okuma, K. Kawabata, K. Shiozaki, M. Sato, *Phys. Rev. Lett.* **2020**, 124, 086801.
- [74] S. Longhi, *Phys. Rev. Lett.* **2020**, 124, 066602.
- [75] Z. Yang, K. Zhang, C. Fang, J. Hu, *Phys. Rev. Lett.* **2020**, 125, 226402.
- [76] L. Xiao, T. Deng, K. Wang, G. Zhu, Z. Wang, W. Yi, P. Xue, *Nature Phys.* **2020**, 16, 761.
- [77] A. Ghatak, M. Brandenbourger, J. van Wezel, C. Coulais, *Proc Nat. Acad. Sci.* **2020**, 117, 29561.
- [78] T. Helbig, T. Hofmann, S. Imhof, M. Abdelghany, T. Kiessling, L.W. Molenkamp, C. H. Lee, A. Szameit, M. Greiter, R. Thomale, *Nature Phys.* **2020**, 16, 747.
- [79] L. E. F. Foa Torres, *J. Phys.: Materials* **2020**, 3, 014002.
- [80] E.J. Bergholtz, J.C. Budich, F.K. Kunst, *Rev. Mod. Phys.* **2021**, 93, 015005.
- [81] K. Wang, A. Dutt, K.Y. Yang, C.C. Wojcik, J. Vuckovic, S. Fan, *Science* **2021**, 371, 1240.
- [82] S. Weidemann, M. Kremer, T. Helbig, T. Hofmann, A. Stegmaier, M. Greiter, R. Thomale, A. Szameit, *Science* **2021**, 368, 311.
- [83] Q. Liang, D. Xie, Z. Dong, H. Li, H. Li, B. Gadway, W. Yi, B. Yan, (Preprint) arXiv:2201.09478, v1, submitted: Jan. **2022**.
- [84] N. Hatano, D.R. Nelson, *Phys. Rev. Lett.* **1996**, it 77, 570.
- [85] S. Longhi, D. Gatti, G. Della Valle, *Sci. Rep.* **2015**, 5, 13376.
- [86] S. Longhi, *Ann. Phys. (Berlin)* **2018**, 530, 1800023.
- [87] N. Hatano, *Physica A* **1998**, 254, 317.
- [88] N. Hatano, T. Watanabe, J. Yamasaki, *Physica A* **2002**, 314, 170.

- [89] S. Longhi, *Phys. Rev. B* **2021**, *104*, 125109.
- [90] A. F. Sadreev, I. Rotter, *J. Phys. A* **2003**, *36*, 11413.
- [91] T. Sandu, A. Chantis, R. Iftimie, *Phys. Rev. B* **2006**, *73*, 075313.
- [92] S. Garmon, M. Gianfreda, N. Hatano, *Phys. Rev. A* **2015**, *92*, 022125.
- [93] S. Longhi, D. Gatti, G. Della Valle, *Phys. Rev. B* **2015**, *92*, 094204.
- [94] S. Longhi, *Phys. Rev. A* **2016**, *93*, 022102.
- [95] K. Lambropoulos, C. Simserides, *J. Phys. Commun.* **2018**, *2*, 035013.
- [96] P.C. Burke, J. Wiersig, M. Haque, *Phys. Rev. A* **2020**, *102*, 012212.
- [97] S. Longhi, *Phys. Rev. Lett.* **2022**, *128*, 157601.
- [98] D.C. Kurtz, *Am. Math. Monthly* **1992**, *99*, 259.
- [99] S. Longhi, *Opt. Lett.* **2010**, *22*, 3844.
- [100] J. K. Asboth, L. Oroszlány, A. Pályi, *A Short Course on Topological Insulators*, Lecture Notes in Physics vol. 919, Springer, Cham, **2016**.
- [101] R. Wang, X. Z. Zhang, Z. Song, *Phys. Rev. A* **2018**, *98*, 042120.
- [102] S. Longhi, *Phys. Rev. B* **2019**, *99*, 155150.
- [103] Y. Yi, Z. Yang, *Phys. Rev. Lett.* **2020**, *125*, 186802.
- [104] Z. Fedorova, H. Qiu, S. Linden, J. Kroha, *Nat. Commun.* **2020**, *11*, 3758.
- [105] H. Schomerus, *Opt. Lett.* **2013**, *38*, 1912.